Original Article

Impact of Respiratory-gated 4D PET/CT Scan for Motion Correction in Characterizing Lesions Adjacent to the Diaphragm – A Cross-sectional Study at a Tertiary Care Institute

Sai Sradha P. Patro, Parag Aland[1], Vivek Mathew James[2], Vikram Lele[3]

Department of Nuclear Medicine, All India Institute of Medical Sciences, Bhubaneswar, Odisha, [1]Department of Nuclear Medicine, Infinity Medical Centre, [3]Department of Nuclear Medicine and Positron Emission Tomography-Computed Tomography, Jaslok Hospital and Research Centre, Mumbai, Maharashtra, [2]Department of Nuclear Medicine, Government Medical College, Thiruvananthapuram, Kerala, India

Abstract

Purpose: The blur introduced by breathing motion degrades the diagnostic accuracy of whole-body F-18 fluorodeoxyglucose positron emission tomography–computed tomography (^{18}F-FDG PET-CT) in lesions adjacent to the diaphragm by increasing the apparent size and by decreasing their metabolic activity. This study aims to evaluate the efficacy of motion correction by four-dimensional phase-based respiratory-gated (RG) ^{18}F-FDG PET-CT in improving metabolic parameters of lesions adjacent to the diaphragm (especially in the lungs or liver). **Materials and Methods:** Eighteen patients with known lung or liver lesions underwent conventional ^{18}F-FDG PET-CT and respiratory-gated PET-CT acquisition of the desired region using a pressure-sensing, phase-based respiratory-gating system. Maximum standardized uptake value (SUV_{max}), metabolic tumor volume (MTV), and total lesion glycolysis (TLG) were obtained for these lesions from gated and nongated PET-CT images for analysis. Furthermore, a visual analysis of lesions was done. **Statistics:** Statistical significance of the RG image parameters was assessed by the two-tailed paired Student's *t* test and confirmed with the robust nonparametric Wilcoxon's signed-rank test (two-tailed asymptotic). **Results:** There was an overall significant increase in SUV_{max} (P 0.001) in all gating methods with a percentage increase maximum of about 18.13%. On gating methods, MTV decreased significantly (P = 0.001) than that of nongating method (maximum reduction of about 32.9%). There was a significant difference (P = 0.02) in TLG between gated and nongated methods. **Conclusion:** Motion correction with phase-based respiratory gating improves the diagnostic value of ^{18}F-FDG PET-CT imaging for lung and liver lesions by more accurate delineation of the lesion volume and quantitation of SUV and can thus impact staging, diagnosis as well as management in selected patients.

Keywords: *Anzai pressure sensors, gated positron emission tomography–computed tomography, phase-based respiratory gating, Q.Freeze, Q.Static*

Introduction

F-18 fluorodeoxyglucose positron emission tomography (F-18 FDG PET) is widely used in oncological imaging for diagnosis and metastatic workup because the proliferating cancer cells have a higher rate of glucose metabolism (measured as standard uptake value-SUV). Hybrid imaging by integrating 18F-FDG PET with computed tomography (CT) has incremental value, combining metabolic and anatomical information. The metabolic information of FDG PET is useful in characterizing indeterminate lung nodules on CT. Accurately localized PET information helps to diagnose and manage patients with malignant disease.

In sequential whole-body PET/CT acquisition, PET acquisition takes around a few minutes to get enough signal for image reconstruction with positron emission (time-averaged image over many breathing cycles), whereas CT acquisition takes only a few seconds (snapshot of the lesion at one distinct phase of the respiratory cycle). Respiratory motion can cause underestimation of the metabolic activity by about 30% and overestimation of lesion volumes by almost two times or more due to smearing or mismatching.[1]

In case of lung tumors, the magnitude of the motion depends on its dimension (smaller tumor, high mobility) and its location (mobility increases on passing

How to cite this article: Patro SS, Aland P, James VM, Lele V. Impact of respiratory-gated 4D PET/CT scan for motion correction in characterizing lesions adjacent to the diaphragm – A cross-sectional study at a tertiary care institute. Indian J Nucl Med 2024;39:177-84.

Address for correspondence:
Dr. Sai Sradha P. Patro, Department of Nuclear Medicine, All India Institute of Medical Sciences, Bhubaneswar, Odisha, India.
E-mail: drpsaisradha@gmail.com

Received: 14-12-2023
Revised: 08-04-2024
Accepted: 12-04-2024
Published: 17-08-2024

Access this article online

Website: www.ijnm.in
DOI: 10.4103/ijnm.ijnm_142_23
Quick Response Code:

from the upper to the middle, down to the lower lobe).[2] Motion direction is mostly craniocaudal, with magnitude ranging from a few millimeters to 1–3 cm for the lungs and around 1.5–2.5 cm for the liver.[3,4] Respiratory motion blur the images and degrade its contrast due to smearing, leading to overestimation of lesion volume and underestimation of SUV (as mismatching of PET and CT data affects attenuation, proved by phantom studies).[5,6]

Hence, the knowledge of organ and lesion motion is an important factor for diagnosis and management in tumor imaging, as well as for radiotherapy planning, requiring accurate safety margin. Assessment of tumor response also becomes unreliable due to respiratory motions, especially for lung lesions.[7,8]

Phase-based respiratory-gated (RG) PET/four-dimensional (4D) PET is one of the methods to correct the respiratory motion effects on PET-CT. Here, PET data are acquired into discrete bins in synchrony with the breathing phase over a few respiratory cycles using motion sensors. The final image is formed by combining the discrete bins of each respiratory cycle phase by phase. Such short-time bins allow the near-instantaneous tracking of the lesion, thereby resulting in approximately motion-free images using various software reconstructions. Investigators have used different respiratory tracking systems to monitor the respiratory motion, which can be hardware or software systems, that simultaneously generate a trigger during image acquisition at a user-predefined phase.[9]

Different types of external respiration sensors are pressure sensors, spirometers, temperature sensors, and video camera systems. Anzai belt, AZ-733V marketed by Anzai Medical (Tokyo, Japan), is one such pressure-sensing device used for gating.[10-13]

This study aims to analyze the impact of phase-based motion-corrected gated PET/CT on lesions adjacent to the diaphragm using Anzai pressure sensors and various reconstruction software.

Materials and Methods

This was a cross-sectional study, done in a tertiary care institute within a study period of 2 years involving adult cancer patients with liver and lung lesions on PET/CT. This study was conducted after getting institutional ethics committee approval and patient consent.

Patients excluded in this study: pediatric age group, patients with respiratory distress or on any artificial ventilator support, very sick, disoriented, uncooperative or unwilling patients.

Imaging protocol

After at least 4 h of fasting, with measured blood glucose level < 160 mg/dL, patients received an intravenous injection of about 148–185 MBq (4–5 mCi) of F-18 FDG. Whole-body imaging was performed using a combined PET/CT scanner (Discovery PET/CT IQ, GE Healthcare, WI, USA) as per the standard guidelines using the conventional protocol about 55–75 min later, and images were reconstructed.[14]

About 80 min to 120 min after F-18 FDG administration, gated PET and CINE mode CT images (with low radiation dose-10 mA, 120 KVp) of the desired area (chest or upper abdomen) were acquired using a pressure sensor system (AZ7337, Anzai Real-time Position Management, Anzai Medical Systems, Tokyo, Japan). The sensor part consists of an elastic belt, which can be fastened around the patient's abdomen or thorax. During inspiration, increased stress results in increased pressure to the belt. This pressure is then measured by a small load cell, an electronic force sensor placed in a pocket inside the belt. The belt is usually interfaced to a computer, where the change in the pressure, and thus breathing amplitude, is displayed as a function of time. To synchronize the recorded respiratory signal with the list-mode PET acquisition, a custom-built cable is used. When activated, the system issues an end-expiratory trigger signal to start the gated data acquisition in list mode and to mark the beginning and end of the respiratory cycle, which was divided into six equal periods for 5 min. The system works by distributing PET data into each of these bins according to the corresponding temporal phase; for a patient exhibiting rhythmic breathing, the temporal phase corresponds to the position of the thorax in the respiratory cycle [Figure 1a]. Software, i.e. Q.Freeze and Q.Static (by GE Healthcare), were used for image reconstruction of the gated data.

RG (by Q.Freeze and Q.Static software) and nonrespiratory-gated datasets of the desired area were generated from the same time list mode data and compared, instead of the initial whole-body image, which is taken at a different time frame.

Parameters analyzed

Various metabolic parameters of the lesions of interest were analyzed, i.e. maximum standard uptake value (SUV_{max}), metabolic tumor volume (MTV), and total lesion

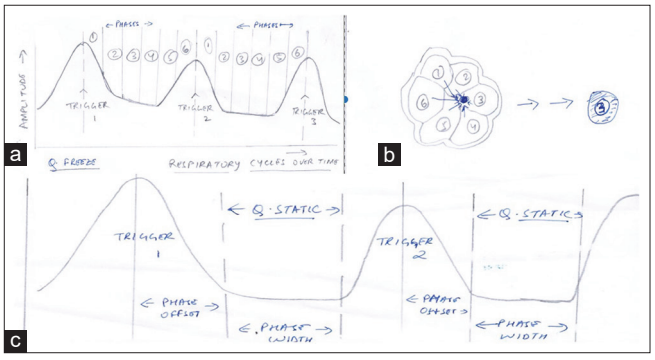

Figure 1: (a) Q.Freeze – Each respiratory cycle data divided into 6 bins. The image formed by coregistration of corresponding bins of all respiratory cycles with quiescent phase as reference. (b) Tumor volumes – nongated (left) versus gated (right). (c) Q.Static – Extract data from the quiescent part of respiratory cycles

glycolysis (TLG). The effect of gating on these parameters was investigated and was compared with nongated images for these lesions.

Software used

Q.Freeze-CINE 4D gated CT in Q.Freeze acquires dynamic CT images at a very low radiation dose (10 mA, 120 Kvp), and six phases of CT are created. PET series acquired over 5 min is gated into a 6-bin dataset. The gated PET is retro-reconstructed using the gated CT into six phases. After retro-reconstructions, a new phase-matched dataset (4D) will be available within the database, which can be viewed using the motion view application in the PET console.

Q.Freeze has been designed to use the entire acquired data to create a single three-dimensional (3D) motion-corrected image/registered image by combining the phase-matched gated frames taking a reference frame or gate for registration [Figure 1b] and provide quantitative accuracy equivalent to 4D phase-matched PET/CT.

Q.Freeze image reconstruction without cycle rejection–(GFCR0)-This combines 100% of the gated PET counts acquired into a 3D motion-corrected image without rejecting any cycle of respiration during acquisition, hence no counts are lost. However, in case of irregular breathing, noise may increase in images.

Q.Freeze image reconstruction with cycle rejection (GFCR1)-3D motion-corrected image is created rejecting the respiratory cycles that are out of phase of the regular breathing cycle of the patient. Images with excess noise due to out-of-phase respiratory cycle were rejected. There is an increased signal-to-noise ratio but there is more count loss if irregular breathing.

Q.Static (GS), also known as quiescent phase gating is designed to extract a fraction of PET data from end-expiratory quiescent portions of patient breathing cycles and form a single 3D PET image volume [Figure 1c]. Thus, there is an increased signal-to-noise ratio. Q.Static software integrates a gating device with an intelligent trigger rejection.

The PET CT review applications on advantage workstations (by GE Healthcare) were used for viewing the images.

Statistics

Data were presented as means ± standard error. Statistical significance was assessed by the two-tailed paired Student's *t*-test and confirmed with the robust nonparametric Wilcoxon's signed-rank test (two-tailed asymptotic): differences with $P < 0.05$ were considered significant and those with $P \leq 0.01$ were considered highly significant. All calculations were performed using statistics software SPSS 20 (SPSS Inc., Chicago, IL, USA).

Results

A total of 18 patients with 55 lesions were analyzed. The mean age of the participants was 56.28 ± 14.05 years. These patients had mostly lung or breast as primary malignancy. Among 55 lesions studied, 65% were in the lungs, 33% were in the liver, and 2% were in the spleen. Ten patients had only lung lesions, four patients had lung and liver lesions, three patients had only liver lesions, and one patient had spleen and lung lesions [Table 1].

There was an overall significant difference in SUV_{max} between different gating methods as compared to nongated method [$P < 0.001$, Tables 2-6]. On gating methods, there was a higher SUV_{max} than that of nongating method. The percentage increase in SUV_{max} was 7.74% (with GFCR0), 18.13% (with GFCR1), and 13.22% (with GS) in gated images.

There was a significant difference in MTV between different gating methods as compared to nongated method ($P < 0.001$). MTV was less on gating methods than that of nongating method. The percentage decrease of MTV was 18.3% (with GFCR0), 32.9% (with GFCR1), and 15.4% (with GS) in gated images. There was a significant difference in TLG in GFCR1 and GS as compared with nongated method [$P = 0.02$, Tables 2-6].

In this study, among the three gating methods, Q.Freeze data with cycle rejection (GFCR1) showed the highest increase in SUV_{max} (18.13%) and reduction in MTV (32.9%), but the problem with few cases was more rejection of cycles causing count loss and excess noise. This caused to exclude these few cases in overall statistical calculation for comparison with other methods affecting the overall parameters of GFCR1 [Table 1].

Discussion

Overall, in comparison with nongating (G0) method, there was a significant increase in SUV_{max} ($P < 0.001$) in all gating methods in this study. A review article has quoted the maximum increase in SUV_{max} to be 83.3% with a maximum increase for small lung lesions (<10 mm) and those located near the diaphragm.[15] This review also summarized that RG improved the diagnostic performance of PET/CT for equivocal lung nodules (i.e. improved Sn, Sp, and accuracy). SUV is lower when a tracer-avid feature is moving during acquisition because the number of events is distributed over a larger volume of interest. Hence, RG should result in higher SUV_{max} which is demonstrated in our study results.

FDG PET/CT has found its way into oncologic treatment planning as another method for the determination of gross MTV of primary tumors and metastases.[16] However, respiratory motion of intrapulmonary lesions leads to an erroneous larger target irradiation area causing more damage to healthy surrounding lung tissue.[17] Breath-hold

Table 1: Lesion characteristics and its quantitative parameters in gated and nongated images in each patient

Patient number	Lesion number	Organ	SUV_ G0	MTV_ G0	TLG_ G0	SUV_ GFCR0	MTV_ GFCR0	TLG_ GFCR0	SUV_ GFCR1	MTV_ GFCR1	TLG_ GFCR1	SUV_ GS	MTV_ GS	TLG_ GS
1	1	RtLLL	6.03	2.9	11.06	5.7	4.07	14.71	6.63	2.7	11.59	6.49	2.5	9.31
	2	RtLLL	7.67	1.52	6.5	7.76	0.99	5.08	8.2	1.13	5.84	6.57	1.6	6.33
2	3	LtLLL	12.79	6.54	47.81	10.82	7.8	48.48	14.48	3.64	28.86	13.34	5.37	42.12
	4	RtLUL	3.4	0.78	1.7	2.71	0.82	1.43	#	#	#	4.5	0.43	1.27
3	5	LtLLL	16.3	8.06	83.59	18.38	7.97	89.04	#	#	#	18.26	7.4	82.98
	6	LTLLL	13.42	0.6	4.56	12.25	0.69	5.3	#	#	#	13.58	0.5	5.07
	7	LtLLL	9.13	0.6	3.28	7.62	0.65	3.33	#	#	#	9.84	0.47	2.99
	8	LtLLL	6.19	2.04	7.15	6.68	1.43	5.82	#	#	#	6.14	1.86	6.89
	9	LtLUL	19.9	1.65	22.23	22.3	1.3	20.43	#	#	#	22.26	1.34	20.66
	10	RtLLL	18.98	1.13	12.94	18.25	1.21	14.46	#	#	#	19.26	0.95	11.11
	11	RtLLL	13.07	11.4	88.55	13.34	9.49	76.81	#	#	#	16.58	7.63	70.61
	12	LtLLL	11.63	4.3	34.25	11.77	4.81	39	#	#	#	16.97	3.08	28.83
4	13	LtLLL	6.29	0.34	1.63	6.46	0.47	2.08	7.15	0.39	1.72	6.44	0.39	1.65
	14	Liver	5.96	28.08	99.61	7.29	16.9	69.68	8.16	13.22	60.05	6.94	20.67	81.76
5	15	Liver	11.83	1.47	11.16	12.43	1.26	10.54	12.84	1.3	10.69	13.95	1.17	10.2
	16	Liver	5.93	9.36	32.17	6.57	5.46	20.93	7.07	5.81	22.79	5.84	7.06	26.27
	17	Liver	10.62	2.64	15.83	13.01	1.6	13.39	11.43	2.56	18.1	11.85	2.21	16.52
	18	Liver	15.8	61.79	614.9	19.6	45.59	531.29	21.53	42.77	521.21	17.15	57.76	607.65
6	19	LtLLL	2.12	1.8	2.36	2.25	1.73	2.23	#	#	#	#	#	#
7	20	RtLLL	9.22	4.03	21.64	10.31	3.64	22.6	11.14	2.95	19.64	9.02	4.33	24.35
8	21	LtLLL	4.2	0.99	2.45	5.64	0.82	3.22	5.92	0.73	3.04	5.06	0.78	2.68
	22	RtLLL	10.06	16.94	110.33	10.58	16.29	112.42	10.49	16.47	113.05	9.72	16.99	109.57
9	23	Liver	6.2	4.2	14.7	7.18	2.69	11.26	11.3	0.82	6.14	8.31	1.18	8.57
	24	Liver	5.73	3.12	10.39	5.91	2.86	9.89	7.01	1.99	8.79	5.96	2.9	9.79
	25	Liver	10.74	3.38	20.89	9.67	4.07	24.82	10.08	3.64	21.61	11.13	3.16	20.12
	26	Liver	6.49	6.98	24.23	6.94	6.24	23.91	10.53	1.21	7.26	7.01	5.63	21.22
	27	Liver	8.04	1.95	9.15	8.18	1.39	7.24	8.33	1.43	7.57	9.4	1.34	7.53
	28	Liver	4.29	6.24	16.21	4.64	5.55	15.09	5.46	3.64	10.95	4.88	5.33	15.18
10	29	LtLLL	7.77	3.16	15.087	7.74	4.42	22.66	#	#	#	8.41	2.77	13.67
11	30	SPLEEN	12.22	0.91	6.87	13.42	0.78	6.86	13.48	0.73	6.73	16.31	0.6	6.21
	31	RtLLL	8.41	1.6	8.58	8.99	1.34	8.18	9.1	1.39	8.4	8.93	1.26	7.41
	32	RtLUL	5.9	7.15	25.37	7.4	5.16	21.55	6.97	5.89	23.88	5.61	7.97	27.15
12	33	Liver	7.01	4.29	17.93	7.74	3.47	16.27	9.6	2.95	16.39	11.26	2.51	15.6
	34	Liver	5.99	3.21	11.63	6.52	2.9	11.62	7.89	1.99	9.01	10.34	1.17	6.92
13	35	LtLUL	11.05	0.78	4.94	12.91	0.43	3.37	12.82	0.43	3.38	13.18	0.43	3.54
	36	LtLUL	9.09	1.13	6.69	10.6	0.95	6.67	10.68	0.95	6.68	10.47	0.86	5.97
	37	LtLLL	12.52	1.47	12.21	12.9	1.73	14.74	12.9	1.69	14.52	11.69	1.73	13.17
	38	LtLUL	3.7	3.25	7.2	5.54	1.34	4.46	5.54	1.34	4.45	5.34	1.04	3.48
	39	RtLLL	2.75	5.94	10.2	4.13	2.82	6.52	4.17	2.6	6.14	3.55	1.99	4.4
14	40	RTLML	9.92	1.08	7.04	10.68	1.04	7.03	10.68	1.04	7.03	10.91	1.14	7.59
	41	RTLML	7.82	0.52	2.7	7.97	0.56	2.98	7.97	0.6	3.14	7.43	0.69	3.27
	42	LtLLL	2.87	2.83	5.06	3.52	2.34	5.13	3.52	2.17	4.99	3.77	1.52	3.49
15	43	RtLML	6.8	2.9	12.24	7.12	1.86	7.97	7.97	1.73	7.83	6.85	2.95	12.28
16	44	LtLUL	21.49	0.86	11.87	22.49	0.82	11.4	25.08	0.69	10.61	20.87	0.91	13.15
	45	LtLLL	8.19	0.26	1.46	9.35	0.52	3.05	8.83	0.56	3.25	14.46	0.13	1.46
	46	RtLLL	7.94	2.25	10.7	11.74	1.34	9.48	12.59	1.21	8.85	12.74	0.65	5.28
	47	RtLLL	10.98	1.3	8.15	11.79	1.95	14.56	13.59	1.56	12.7	14.11	1.04	8.7
	48	Liver	12.22	2.21	16.96	13.86	1.43	12.71	15.81	1.3	12.55	14.25	1.73	15.87
	49	Liver	15.53	12.39	129.07	16.42	11.01	124.94	16.42	11.01	124.94	18.12	10.4	122.76
	50	Liver	11.65	0.82	5.93	10.7	1.13	7.94	#	#	#	16.4	0.56	5.25
17	51	RtLUL	2.45	5.5	8.39	3.03	3.55	6.25	#	#	#	2.97	4.55	7.58

Contd...

Table 1: Contd...

Patient number	Lesion number	Organ	SUV_ G0	MTV_ G0	TLG_ G0	SUV_ GFCR0	MTV_ GFCR0	TLG_ GFCR0	SUV_ GFCR1	MTV_ GFCR1	TLG_ GFCR1	SUV_ GS	MTV_ GS	TLG_ GS
18	52	LtLLL	5.79	1.21	4.25	8.4	0.69	3.31	#	#	#	5.79	1.21	4.25
	53	Liver	26.47	18.8	294.47	26.52	18.89	304.24	#	#	#	26.47	18.81	294.47
	54	Liver	23.81	2.47	38.96	25.91	2.34	39.87	#	#	#	23.81	2.47	38.96
	55	Liver	10.69	2.25	15.19	12.77	1.99	16.68	#	#	#	10.69	2.25	15.19

#: Corresponding gating parameters could not be assessed for these lesions due to count loss by cycle rejection in irregular breathing, RtLLL: Right lung lower lobe, RtLUL: Right lung upper lobe, LtLLL: Left lung lower lobe, LtLUL: Left lung upper lobe, RTLML: Right lung middle lobe, MTV: Metabolic tumor volume, SUV: Standardized uptake value, TLG: Total lesion glycolysis

Table 2: Comparison of maximum standardized uptake value, metabolic tumor volume, and total lesion glycolysis measured using gated (GFCR0-Q freeze without cycle rejection) with nongating method (*n*=55)

Parameters	Mean±SD		*P**
	Nongated	Gated (GFCR0)	
SUV_{max}	9.69±5.3	10.44±5.52	<0.001
MTV	5.14±9.26	4.2±6.95	<0.01
TLG	36.43±91.46	33.88±81.91	0.139

*Student's *t*-pair test was used, $P \leq 0.05$ significant. MTV: Metabolic tumor volume, SUV_{max}: Maximum standardized uptake value, TLG: Total lesion glycolysis, SD: Standard deviation

Table 3: Comparison of maximum standardized uptake value, metabolic tumor volume, and total lesion glycolysis measured using gated (GFCR1-Q freezing with cycle rejection) with nongating method (*n*=39, images with excess noise due to cycle rejection were excluded from the study)

Parameters	Mean±SD		*P**
	Nongated	Gated (GFCR1)	
SUV_{max}	8.77±3.85	10.36±4.34	<0.001
MTV	5.56±10.56	3.73±7.2	<0.001
TLG	35.05±98.85	29.24±83.30	0.03

*Student's *t*-pair test was used, $P \leq 0.05$ significant. MTV: Metabolic tumor volume, SUV_{max}: Maximum standardized uptake value, TLG: Total lesion glycolysis, SD: Standard deviation

techniques are compromised if patients cannot comply with breathing instructions, which can be a problem in lung cancer patients. Robin *et al*., in their study, found a significant reduction of MTV (18%) and TLG with gating which is also found in our study.[18] This improvement is important in treatment planning before radiation therapy to define the irradiation target volume more accurately.[19] The visual blur in the static image resulting from respiratory motion generally appears stretched along the direction of the motion and can be quantified by tumor volume change [Figure 2].

Both phantom and retrospective clinical studies have demonstrated superior image quality and increased accurate quantitative parameters in gated images compared to conventional static images.[20,21]

Table 4: Comparison of maximum standardized uptake value, metabolic tumor volume, and total lesion glycolysis measured using gated (GS-Q static) with nongating method (*n*=54)

Parameters	Mean±SD		*P**
	Nongated	Gated (GS)	
SUV_{max}	9.83±5.26	11.13±5.54	<0.001
MTV	5.20±9.33	4.40±8.61	<0.001
TLG	37.06±92.20	35.52±91.52	0.02

*Student's *t*-pair test was used, $P \leq 0.05$ significant. MTV: Metabolic tumor volume, SUV_{max}: Maximum standardized uptake value, TLG: Total lesion glycolysis, SD: Standard deviation

Majority of patients tend to spend more breathing time dwelling at the end-expiration quiescent period and breathe out to the same end-expiratory location. These results indicate that imaging at end-expiration could involve less motion while still retaining a large fraction of the PET data.

Q.Static (GS), known as quiescent phase gating, extracts a fraction of PET data from end-expiratory quiescent portions of patient breathing cycles and forms a single 3D PET image volume. Thus, there is an increased signal-to-noise ratio. It is an automated motion correction method that can be integrated into the clinical whole-body PET protocol and provides motion-corrected images of the desired area after reconstruction simultaneously with the conventional PET acquisition and reconstruction. Thus is more convenient to use in regular clinical practice.

RG improves the accuracy in assessment of upper abdominal lymph node involvement. In one patient in this study, new tiny avid lymph nodes in the abdomen were identified on gated image which was not detected in ungated image [Figure 3a and b]. New lung nodules were also found after gating in two patients which were not appreciated in nongated study [Figure 3c and d]. Even non-FDG-avid lung nodule on nongated image showed FDG uptake on gated study [Figure 3e and f]. Hence, it suggests that gating could facilitate the detection of very small lesions which has a major impact on diagnosis, management, and staging.[22] The sharpness of the margins of the lung nodules is also better than nongated images, particularly those at interface of the lung and diaphragm, confusing as liver lesions [Figure 4a and b].[23]

Table 5: Comparison of measurement of standardized uptake value in supradiaphragmatic lesion

Parameters	Mean±SD			*P** (*n*1 vs. *n*2 vs. *n*3)
	Nongated versus GFCR0 (*n*1=36)	Nongated versus GFCR1 (*n*2=36)	Nongated versus GS (*n*3=36)	
SUV_{max}	9.10±4.84 versus 9.76±4.93	8.59±4.05 versus 9.97±4.52	9.30±4.76 versus 10.43±5.20	0.001 versus<0.001 versus 0.001
MTV	3.06±3.45 versus 2.73±3.24	2.96±3.61 versus 2.31±3.33	3.09±3.50 versus 2.56±3.28	0.040 versus 0.004 versus 0.004
TLG	17.65±25.48 versus 17.67±25.46	15.08±22.99 versus 13.92±22.67	18.08±25.71 versus 16.64±24.3	0.96 versus 0.21 versus 0.02

*Student's *t*-pair test was used, (GFCR0-Q freezing without cycle rejection, GFCR1-Q freezing with cycle rejection, GS-Q static), $P \leq 0.05$ significant. MTV: Metabolic tumor volume, SUV_{max}: Maximum standardized uptake value, TLG: Total lesion glycolysis, SD: Standard deviation

Table 6: Comparison of measurement of standardized uptake values in infradiaphragmatic lesion

Parameters	Mean±SD			*P** (*n*1 vs. *n*2 vs. *n*3)
	Nongated versus GFCR0 (*n*1=36)	Nongated versus GFCR1 (*n*2=36)	Nongated versus GS (*n*3=36)	
SUV_{max}	10.81±6.09 versus 11.73±6.45	9.02±3.67 versus 10.93±4.15	10.81±6.09 versus 12.42±6.02	0.003 versus 0.001 versus 0.001
MTV	9.07±14.45 versus 6.97±10.59	9.30±15.43 versus 5.77±10.37	9.07±14.45 versus 7.77±13.4	0.04 versus 0.02 versus 0.008
TLG	72.03±147.61 versus 64.60±131.7	63.74±149.96 versus 51.27±127.13	72.03±147.61 versus 70.3±146.89	0.130 versus 0.05 versus 0.286

*Student's *t*-pair test was used, (GFCR0-Q freezing without cycle rejection, GFCR1-Q freezing with cycle rejection, GS-Q static), $P \leq 0.05$ significant. MTV: Metabolic tumor volume, SUV_{max}: Maximum standardized uptake value, TLG: Total lesion glycolysis, SD: Standard deviation

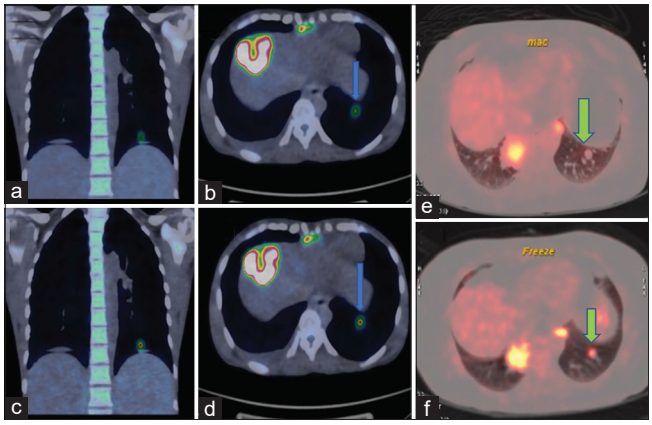

Figure 2: (a and b) Nongated coronal and axial images of the left lung nodule appear blurred (arrow). (c and d) Gated images – the lesion is better delineated with increased SUV (arrow). (e) Nonavid left lung nodule near diaphragm on nongated image shows avidity on the gated image (arrow) (f)

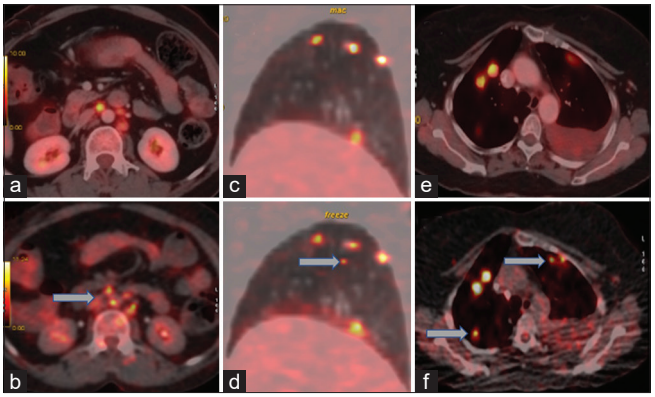

Figure 3: (a, c and e) Nongated axial and sagittal images and (b, d and f) its corresponding gated images. Few new FDG-avid abdominal lymph nodes and lung nodules were detected/better appreciated after respiratory gating (arrows in b, d and f)

Liver lesions are also affected by respiratory movement which on fused PET-CT images appear blurred and smeared. Physiological uptake of the surrounding liver parenchyma under voluntary respiration also affects the assessment of the lesions which are better appreciated with gating [Figure 4c and d]. Therefore, this feasibility study shows RG PET/CT images having higher SUV_{max} and lower MTV in liver lesions [Table 1]. A similar diagnostic performance was reported by Cheung *et al*.[24]

The results of our study suggest that RG improves the semi-quantitative assessment of lesions adjacent to the diaphragm on PET/CT. Although some additional time and training are needed for setup and acquisition, RG can be incorporated practically and efficiently into clinical routines. New PET/CT scanners have fully automatic processes for RG data sorting and image reconstruction (like the Q.Static software), making the RG technique feasible in routine clinical setting. 4D phase-based RG using Q.Freeze should be reserved for truly equivocal cases when the detection and true FDG activity of a lesion in the lower thorax or upper abdomen would likely influence the clinical management of the patient, like for staging or planning targeted therapy. RG also has the potential for providing accurate measurements of metabolic parameters for targeted therapy, monitoring of the therapeutic response, assessment of tumor viability,

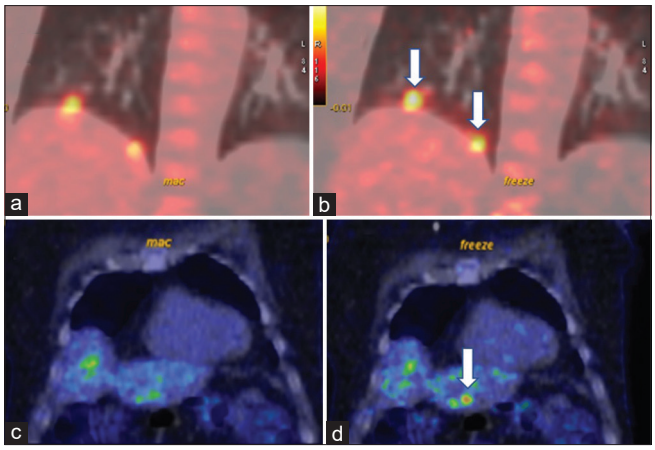

Figure 4: (a) Nongated sagittal image, (b) Gated image. The lung nodule which was smeared with the liver surface is seen separately after gating (arrows). (c) Nongated coronal image, (d) Gated image. A liver lesion better detected after respiratory gating (arrow)

textural analysis, and prognostication. It is likely to be an important component of further future advancements in molecular imaging, where the highest spatial resolution and sensitivity are desired. Further extensive studies are needed to define the impact of these improvements on diagnosis, radiation therapy planning, therapy monitoring, and textural analysis.[25] The major limitations to widespread clinical adoption of respiratory motion correction to date are the need for extra acquisition, need for training, and expertise for the external device-driven RG. This can be eliminated if RG can be incorporated directly in initial image acquisition, which seems possible with Q.Static software. Messerli *et al*., studied feasibility of using data-driven RG [DDG] with Q.Static, showing promising results impacting clinical management.[26] DDG PET/CT also showed more accurate quantification of lung and upper abdomen lesions in another study.[27]

The limitation of this study is that the number of patients included is relatively small. This was due to the heavy workload of the department to acquire another study for the patient and difficulty in training the patient for regular respiration. Furthermore, since the patients analyzed in this study had multiple metastatic lesions, the data did not significantly impact the management but would definitely be useful for follow-up/response evaluation. A larger-scale and prospective investigation to assess the clinical impact of RG PET/CT is required.

Conclusion

From this study, it is concluded that RG improves the quality of PET imaging in lesions adjacent to the diaphragm as well as its quantification and feasible in routine clinical practice for selected patients who would be benefited. We have shown that image smearing can be reduced by phase-based motion-corrected RG FDG PET/CT. This technique allows a more accurate definition of the metabolic parameters with the identification of new lesions, useful for diagnosis, staging, treatment, prognostication, and response evaluation. It is also useful to differentiate between lung and liver lesions near the diaphragm further impacting clinical decision and management.

Acknowledgment

We would like to thank Mr. Laxman Khande, senior technologist, JHRC, and Mr. Swatantramani Dubey, GE Healthcare engineer.

Financial support and sponsorship

Nil.

Conflicts of interest

There are no conflicts of interest.

References

1. Liu C, Pierce LA 2nd, Alessio AM, Kinahan PE. The impact of respiratory motion on tumor quantification and delineation in static PET/CT imaging. Phys Med Biol 2009;54:7345-62.
2. Keall PJ, Mageras GS, Balter JM, Emery RS, Forster KM, Jiang SB, *et al.* The management of respiratory motion in radiation oncology report of AAPM Task Group 76. Med Phys 2006;33:3874-900.
3. Shirato H, Seppenwoolde Y, Kitamura K, Onimura R, Shimizu S. Intrafractional tumor motion: Lung and liver. Semin Radiat Oncol 2004;14:10-8.
4. Seppenwoolde Y, Shirato H, Kitamura K, Shimizu S, van Herk M, Lebesque JV, *et al.* Precise and real-time measurement of 3D tumor motion in lung due to breathing and heartbeat, measured during radiotherapy. Int J Radiat Oncol Biol Phys 2002;53:822-34.
5. Nehmeh SA, Erdi YE, Ling CC, Rosenzweig KE, Schoder H, Larson SM, *et al.* Effect of respiratory gating on quantifying PET images of lung cancer. J Nucl Med 2002;43:876-81.
6. Pevsner A, Nehmeh SA, Humm JL, Mageras GS, Erdi YE. Effect of motion on tracer activity determination in CT attenuation corrected PET images: A lung phantom study. Med Phys 2005;32:2358-62.
7. Kim DJ, Murray BR, Halperin R, Roa WH. Held-breath self-gating technique for radiotherapy of non-small-cell lung cancer: A feasibility study. Int J Radiat Oncol Biol Phys 2001;49:43-9.
8. Chen QS, Weinhous MS, Deibel FC, Ciezki JP, Macklis RM. Fluoroscopic study of tumor motion due to breathing: Facilitating precise radiation therapy for lung cancer patients. Med Phys 2001;28:1850-6.
9. Nehmeh SA, Erdi YE, Ling CC, Rosenzweig KE, Squire OD, Braban LE, *et al.* Effect of respiratory gating on reducing lung motion artifacts in PET imaging of lung cancer. Med Phys 2002;29:366-71
10. Kubo HD, Hill BC. Respiration gated radiotherapy treatment: A technical study. Phys Med Biol 1996;41:83-91.
11. Dietrich L, Jetter S, Tücking T, Nill S, Oelfke U. Linac-integrated 4D cone beam CT: First experimental results. Phys Med Biol 2006;51:2939-52.
12. Martínez-Möller A, Bundschuh R, Riedel M, Navab N, Ziegler S, Schwaiger M, *et al*. Comparison of respiratory sensors and its compliance for respiratory gating in emission tomography.Proceedings of annual meeting of society of nuclear medicine, Washington, DC, June 2007. J Nucl Med 2007;48:426.

13. Guivarc'h O, Turzo A, Visvikis D, Bizais Y. Synchronization of pulmonary scintigraphy by respiratory flow and by impedance plethysmography. In Medical Imaging 2004: Image Processing 2004,12 (Vol. 5370, pp. 1166-75).
14. Boellaard R, Delgado Bolton R, Oyen WJ, Giammarile F, Tatsch K, Eschner W, *et al.* FDG PET/CT: EANM procedure guidelines for tumour imaging: Version 2.0. Eur J Nucl Med Mol Imaging 2015;42:328-54.
15. Crivellaro C, Guerra L. Respiratory gating and the performance of PET/CT in pulmonary lesions. Curr Radiopharm 2020;13:218-27.
16. Nehmeh SA, Erdi YE. Respiratory motion in positron emission tomography/computed tomography: A review. Semin Nucl Med 2008;38:167-76.
17. Guckenberger M, Krieger T, Richter A, Baier K, Wilbert J, Sweeney RA, *et al.* Potential of image-guidance, gating and real-time tracking to improve accuracy in pulmonary stereotactic body radiotherapy. Radiother Oncol 2009;91:288-95.
18. Robin P, Bourhis D, Bernard B, Abgral R, Querellou S, Le Duc Pennec A, *et al.* Feasibility of systematic respiratory-gated acquisition in unselected patients referred for 18F-fluorodeoxyglucose positron emission tomography/computed tomography. Front Med (Lausanne) 2018;5:36.
19. Lupi A, Zaroccolo M, Salgarello M, Malfatti V, Zanco P. The effect of 18F-FDG-PET/CT respiratory gating on detected metabolic activity in lung lesions. Ann Nucl Med 2009;23:191-6.
20. Wollenweber SD, Gopalakrishnan G, Thielemans K, Manjeshwar RM. Evaluation of the accuracy and robustness of a motion correction algorithm for PET using a novel phantom approach. IEEE Transactions on Nuclear Science. 2012;59:123-30.
21. De Ponti E, Guerra L, Morzenti S, Elisei F, Zorz A, Crivellaro C, *et al*. A new algorithm (MotionFreeze-MF) for respiratory motion management in PET/CT scan: Comparison to respiratory gated PET/CT (4D) data.SNM Annu Meet Abstr 2012;53:2378.
22. Grootjans W, Hermsen R, van der Heijden EH, Schuurbiers-Siebers OC, Visser EP, Oyen WJ, *et al.* The impact of respiratory gated positron emission tomography on clinical staging and management of patients with lung cancer. Lung Cancer 2015;90:217-23.
23. Sarikaya I, Yeung HW, Erdi Y, Larson SM. Respiratory artefact causing malpositioning of liver dome lesion in right lower lung. Clin Nucl Med 2003;28:943-4.
24. Cheung AH, Wu VW, Cheung AL, Cai J. Respiratory 4D-gating F-18 FDG PET/CT scan for liver malignancies: Feasibility in liver cancer patient and tumor quantitative analysis. Front Oncol 2022;12:789506.
25. Hatt M, Tixier F, Visvikis D, Cheze Le Rest C. Radiomics in PET/CT: More than meets the eye? J Nucl Med 2017;58:365-6.
26. Messerli M, Liberini V, Grünig H, Maurer A, Skawran S, Lohaus N, *et al*. Clinical evaluation of data-driven respiratory gating for PET/CT in an oncological cohort of 149 patients: impact on image quality and patient management. Br J Radiol. 2021,1;94:20201350.
27. Kang SY, Moon BS, Kim HO, Yoon HJ, Kim BS. The impact of data-driven respiratory gating in clinical F-18 FDG PET/CT: Comparison of free breathing and deep-expiration breath-hold CT protocol. Ann Nucl Med 2021;35:328-37.